Synchronization of driven nonlinear oscillators

R. V. Jensen[a)]
Department of Physics, Wesleyan University, Middletown, Connecticut 06459

(Received 22 June 2001; accepted 18 December 2001)

Mathematical models of nonlinear oscillators are used to describe a wide variety of physical and biological phenomena that exhibit self-sustained oscillatory behavior. When these oscillators are strongly driven by forces that are periodic in time, they often exhibit a remarkable ''mode-locking'' that synchronizes the nonlinear oscillations to the driving force. The purpose of this paper is to demonstrate that a similar phenomenon occurs when nonlinear oscillators are strongly driven by a force that is varying randomly in time. In this case the synchronization is less obvious for a single oscillator, but when several oscillators with different initial conditions or phases are driven with the same aperiodic force, their fluctuating behavior may reliably converge to an identical response. Analytical estimates are derived for the conditions, rates, and structural stability for the synchronization of a broad class of aperiodically driven nonlinear oscillators. © *2002 American Association of Physics Teachers.*

[DOI: 10.1119/1.1467909]

I. INTRODUCTION

A very old and important result in nonlinear dynamics is that when nonlinear oscillators with stable limit cycles are subject to periodic perturbations, these oscillators may become entrained to the perturbation. This phenomenon of ''mode-locking'' or ''phase-locking'' is epitomized by Huygens' ancient observation that pendulum clocks hung from the same beam tend to synchronize due to the common periodic vibrations of the beam.[1] This effect has several important manifestations. A driven nonlinear oscillator may be ''entrained'' to oscillate at the same frequency as the periodic driving force,[2–6] the periodic perturbation can synchronize two identical nonlinear oscillators with different initial conditions,[3,7] and two coupled oscillators can periodically drive each other to a common phase-locked state.[2,3]

The purpose of this paper is to describe how similar phenomena occur when nonlinear oscillators are subject to perturbations that fluctuate randomly in time. A signature of this random phase-locking is provided when two aperiodically driven nonlinear oscillators with different initial conditions are observed to reliably converge to asymptotically identical, synchronized states. In the mathematical literature this reliable synchronization of dynamical systems is known as ''asymptotic stability''.[6]

For stable (damped), linear oscillators, asymptotic stability is a trivial result for both periodic and aperiodic driving forces.[6] Consider, for example, the equation of motion for the position, x, of a particle of mass unity, connected to a linear spring with frequency, Ω, in a viscous medium with linear drag coefficient, γ, subject to a fluctuating driving force, $F(t)$,

$$\frac{d^2x}{dt^2} = -\gamma\frac{dx}{dt} - \Omega^2 x + F(t). \tag{1}$$

The standard solution of this linear differential equation shows that, for any initial condition, $x(0)$ and $\dot{x}(0)$, the long-time behavior converges to the same particular solution of the differential equation at a rate γ. In addition, the convergence to a common solution is ''structurally stable'' in the sense that small changes in the parameters of the linear oscillator or in the driving force would result only in small changes in the asymptotic behavior.

However, for nonlinear differential equations, such as the driven van der Pol oscillator,[3–6]

$$\frac{d^2x}{dt^2} = \epsilon(1-x^2)\frac{dx}{dt} - \Omega^2 x + F(t), \tag{2}$$

the conditions for asymptotic stability are very much dependent on the parameters of the nonlinear system and the properties of the driving force. Although there is a vast literature on this subject,[3–6] there are few analytical results. Qualitatively, mode-locking occurs when the periodic driving force is sufficiently strong and the frequency of the force is sufficiently close to the unperturbed frequency of the nonlinear oscillator. For example, in Fig. 1(a) we show for $\Omega=1$, $\epsilon=1$, and $F(t)=B\sin\omega t$ with $B=0.5$ and $\omega=1.05$ that the numerical solutions for $x_1(t)$ and $x_2(t)$ with initial conditions, $x_1(0)=1$ and $x_2(t)=-1$ [with $\dot{x}_{1,2}(0)=0$] converge rapidly to synchronized, mode-locked behavior.

In this case the rate of asymptotic convergence can be measured from the negative average slope of

$$r_{\rm syn}(t) = \log(|x_1(t)-x_2(t)|/|x_1(0)-x_2(0)|), \tag{3}$$

as shown in Fig. 1(b). However, if the driving frequency is shifted further away from the natural frequency, $\Omega=1$, to $\omega=1.1$ or B is reduced from $B=0.5$ to $B=0.3$, the numerical solutions of Eq. (2) no longer converge to a common mode-locked solution and $r_{\rm syn}(t)$ simply oscillates around a constant value with zero average slope.

Although anticipated by earlier work by Pikovsky,[8] the synchronization of two van der Pol oscillators by an aperiodic drive, $F(t)=B\sin\phi_r(t)$ with random phase $\phi_r(t)$, was a surprise [see Fig. 2(a)].[9] In this case it is not clear to what the oscillator is mode-locking, because the driven oscillator also exhibits random fluctuations. Nevertheless, the asymptotic rate of convergence can be determined by the negative average slope of $r_{\rm syn}(t)$ as shown in Fig. 2(b).

A wide variety of different nonlinear oscillators in the physical and biological sciences, from the van der Pol equations for nonlinear electrical circuits to the Hodgkin–Huxley equations for neuronal dynamics, can be shown to exhibit

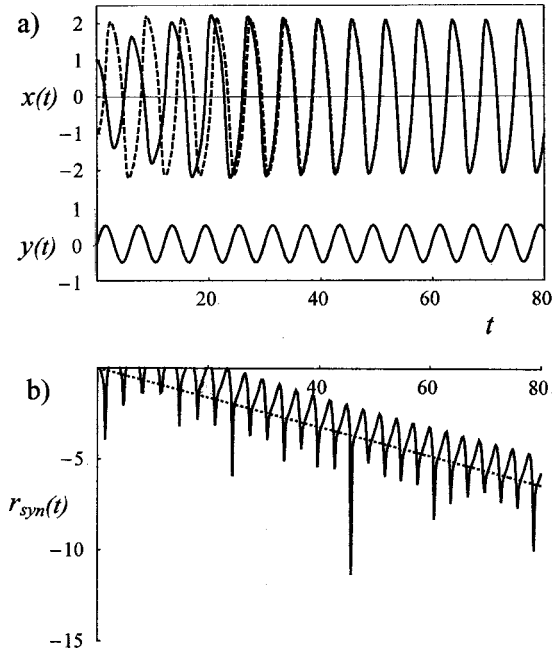

Fig. 1. (a) Plot of the displacement $x(t)$ of two periodically driven van der Pol oscillators with $\Omega=1$ and $\epsilon=1$. The driving force, $F(t)=0.5\sin 1.05t$, is shown in the lower curve. For the initial conditions, $x_1(0)=1$ (solid line) and $x_2(0)=-1$ (dashed line), the solutions converge to indistinguishable curves by $t=40$. (b) The rate of convergence is determined from the average negative slope of $\langle r_{\rm syn}(t)\rangle\approx -0.08t$ [see Eq. (3)] as indicated by the dotted line.

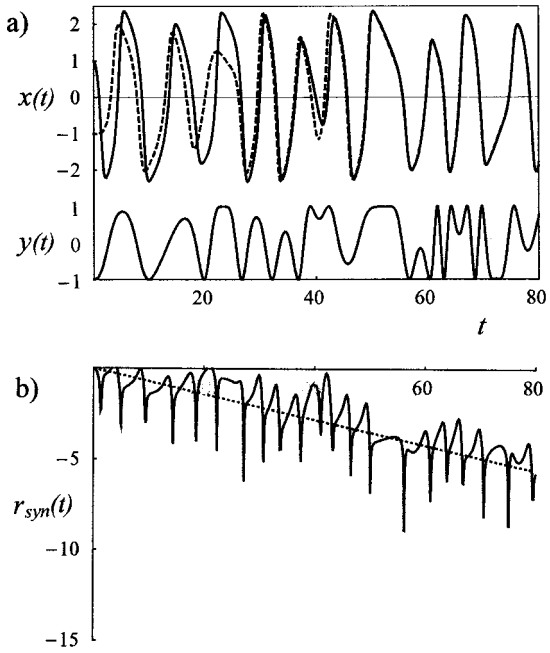

Fig. 2. (a) Plot of $x(t)$ for two randomly driven van der Pol oscillators with $\Omega=1$ and $\epsilon=1$. The driving force, $F(t)=y(t)=1.0\sin\phi_r(t)$, with the Gaussian random phase, $\phi_r(t)$, is shown in the lower curve. For the initial conditions, $x_1(0)=1$ (solid line) and $x_2(0)=-1$ (dashed line), the solutions converge to indistinguishable curves by $t=50$. (b) The rate of convergence is determined from the average negative slope of $\langle r_{\rm syn}(t)\rangle\approx -0.07t$ as indicated by the dotted line.

reliable synchronization when driven by both periodic or aperiodic inputs.[9] Like the periodically driven systems, the synchronization of randomly driven nonlinear oscillators is found to be structurally stable, which means that approximate synchronization is realized even in the presence of small variations (or errors) in the parameters of the systems and small amounts of additional noise in the driving signal. This structural stability is essential for practical applications, because real systems will inevitably have small variations and be subject to additional background noise.

For example, the nonlinear oscillators used to model the spiking, voltage dynamics of neurons, such as the Fitzhugh–Nagumo, Morris–Lecar, and Hodgkin–Huxley equations,[10] are all found to exhibit asymptotically stable, synchronized behavior when strongly driven by randomly fluctuating currents.[11] This effect provides a dynamical mechanism for the remarkable reliability of the spike timing recently observed in the response of neocortical neurons to fluctuating input currents that resemble real synaptically generated currents.[12] The same levels of spike timing reliability are achieved in mathematical models for neuronal oscillations, even with small changes in initial conditions, cell parameters, and driving currents.[11] This reliability of spike timing is essential if single neurons are expected to faithfully encode temporal information in the timing of successive spikes.[13]

Recently, there has been considerable interest in the synchronization of chaotically driven nonlinear systems.[14] For example, in 1990 Pecora and Carrol made the surprising observation that when the fluctuating output of a chaotic system of nonlinear differential equations (transmitter) is used to drive a second nonlinear system consisting of an appropriately chosen subset of the chaotic equations (receiver), the evolution of the driven system would reliably reproduce the behavior of the transmitter.[15] This synchronization of the receiver to the chaotic signal of the transmitter has been widely discussed as a means for secure communication[16] and the control of chaos.[15] However, chaos is not necessary for the realization of this striking effect. Chaotically driven systems are special cases of the more general phenomena of the occurrence of asymptotically stable solutions for aperiodically driven nonlinear systems.

Formally, this stability can be established by constructing an appropriate Lyapunov function or by demonstrating that all of the Lyapunov exponents are negative.[3] However, in practice, rigorous Lyapunov functions can only be constructed in special cases and the negativity of the Lyapunov exponents can only be calculated numerically for specific systems. To build a more useful theoretical foundation for the general phenomenon of the synchronization of nonlinear oscillators by aperiodic inputs, we will focus first on nonlinear oscillators that are well approximated by simple phase models.[17] Analytical expressions are derived to provide quantitative estimates for the conditions for observing synchronization in this broad class of randomly driven nonlinear oscillators as a function of the fluctuation amplitudes and frequency spectra, along with estimates for the rates of convergence to the synchronized solutions and the requirements for structural stability. These results reveal that the synchronization of randomly driven oscillators is closely related to periodically driven oscillators. This correspondence suggests useful experimental procedures for assessing the nonlinear response of biological, chemical, and physical oscillators to fluctuating inputs. Insight into the behavior of nonlinear oscillators subject to natural, aperiodically fluctuating inputs is provided by the empirical characterization of the response to

periodic driving forces. Finally, to demonstrate the success of this procedure, the analytical and empirical results are used to successfully predict the synchronization of randomly driven van der Pol oscillators with moderate and strong nonlinearity.

In Sec. II the simple phase model for a nonlinear oscillator is introduced and the well-studied response of this nonlinear model to a periodic input with constant frequency is reviewed. In Sec. III the stability analysis of the driven phase model is extended to slowly varying drive frequencies. Explicit relations are derived for linearly changing drive frequencies in Sec. III A and for randomly varying drive frequencies in Sec. III B to determine the conditions for asymptotic stability and the rate of convergence toward synchronization. In Sec. IV these results are applied to the venerable van der Pol oscillator. The phase model results are used to predict the conditions for and rates of synchronization caused by both periodically and aperiodically fluctuating drives. Good agreement between the analytical estimates and numerical solutions is demonstrated. Finally, some of the many applications of these results for the synchronization of nonlinear oscillators by aperiodic inputs are briefly reviewed in Sec. V.

II. PHASE MODEL FOR A DRIVEN NONLINEAR OSCILLATOR

Consider two nonlinear oscillators,

$$x(t)=A\sin[\theta(t)], \tag{4}$$

and

$$y(t)=B\sin[\phi(t)], \tag{5}$$

characterized by their phases $\theta(t)$ and $\phi(t)$. For weak coupling, the interaction of these two oscillators can be expressed in terms of the phase differences.[17] For example, a very general form for the response of $\theta(t)$ is provided by the nonlinear phase equation,[2,3,17]

$$\frac{d\theta}{dt}=\Omega-b\sin[\theta(t)-\phi(t)]. \tag{6}$$

If we assume unidirectional coupling from the y oscillator to the x oscillator, the driving phase $\phi(t)$ may be chosen to be an arbitrary function of time. Then the driven phase model defined by Eq. (6) provides a useful toy model for studying the response of nonlinear oscillators to both constant frequency and variable frequency drives. [In Sec. IV the reduction of a driven nonlinear oscillator to the phase model, Eq. (6), is explicitly performed for the van der Pol oscillator.]

Although there is great interest in the collective behavior of large arrays of coupled nonlinear oscillators,[17,18] this paper will focus solely on the response of a single nonlinear oscillator to external forces with constant and variable frequency drives characterized by the time dependence of the driving phase, $\phi(t)$. Moreover, our approach will differ from the traditional[19] studies of the effects of noise on nonlinear oscillators which (typically) assume that the noise is a small perturbation and then rely on a Fokker–Planck type description to provide statistical predictions for the synchronization of the oscillator in the presence of noise. Here, there will be no essential restrictions on the size of the aperiodic or random drive, there will be no Fokker–Planck type approximations, and the synchronization of the nonlinear oscillator due to the strong noise alone will be carefully detailed.

If there is no coupling ($b=0$), then $x(t)=A\sin(\Omega t+\theta_0)$ and simply oscillates at the natural angular frequency Ω starting from the initial phase θ_0. When $b\neq 0$, a variety of different responses are possible due to the competition between Ω and the instantaneous driving frequency, $\omega(t)=\dot{\phi}$.

Constant frequency drive—$\phi(t)=\omega t$

The results for a drive force with constant frequency ω are well known.[3] The position of the driven oscillator, $x(t)$, mode-locks to the drive frequency if b is large enough and ω is close enough to Ω. In this simple model these two requirements are analytically expressed by

$$\left|\frac{\Omega-\omega}{b}\right|<1. \tag{7}$$

When this condition is met, the dynamics of the driven oscillator is asymptotically stable.[6]

This result is easily derived by introducing $\eta(t)=\theta(t)-\omega t$ and rewriting Eq. (6) as

$$\frac{d\eta}{dt}=[\Omega-\omega]-b\sin\eta. \tag{8}$$

The stability criterion, Eq. (7), is consistent with the condition for Eq. (8) to have the asymptotic solution

$$\eta_\infty=\arcsin\left[\frac{\Omega-\omega}{b}\right]. \tag{9}$$

Then the steady-state solution for the driven oscillator phase,

$$\theta(t)\sim\theta_\infty(t)=\omega t+\eta_\infty, \tag{10}$$

describes a mode-locked or phase-locked behavior for

$$x(t)=A\sin(\omega t+\eta_\infty), \tag{11}$$

which oscillates at the frequency of the periodic drive ω with a fixed phase shift, η_∞.

To prove asymptotic stability, it remains to show that starting from two nearby initial conditions, $\theta_1(0)$ and $\theta_2(0)$, $\theta_1(t)$ and $\theta_2(t)$, synchronize at an exponential rate as they converge to the asymptotic solution, Eq. (10). In this simple model the Lyapunov exponent that determines the rate of convergence can be calculated by a simple perturbation analysis based on the linearization of Eq. (8) for small $\delta(t)=\theta_1(t)-\theta_2(t)=\eta_1(t)-\eta_2(t)$:

$$\frac{d\delta}{dt}\approx-b\,\delta\cos[\eta(t)]. \tag{12}$$

If we use Eq. (9) to replace $\eta(t)$ by η_∞ in Eq. (12), we find that the exponential rate of convergence, γ, is given by[3]

$$\gamma=b\cos\eta_\infty=\sqrt{b^2-(\Omega-\omega)^2}, \tag{13}$$

which is real and positive when the inequality in Eq. (7) is satisfied.

One straightforward but important consequence of asymptotic stability is that the long-time behavior of any two driven oscillators, $x_1(t)$ and $x_2(t)$, with initial phases, $\theta_1(0)$ and $\theta_2(0)$, will always *synchronize* [that is, both $|\theta_1(t)-\theta_2(t)|$ and $|x_1(t)-x_2(t)|\sim e^{-\gamma t}$] as $x_1(t)$ and $x_2(t)$ converge (at the exponential rate γ) to their common asymptotic solution.[7] In particular, any difference in the solutions due to different initial conditions will decay exponentially.

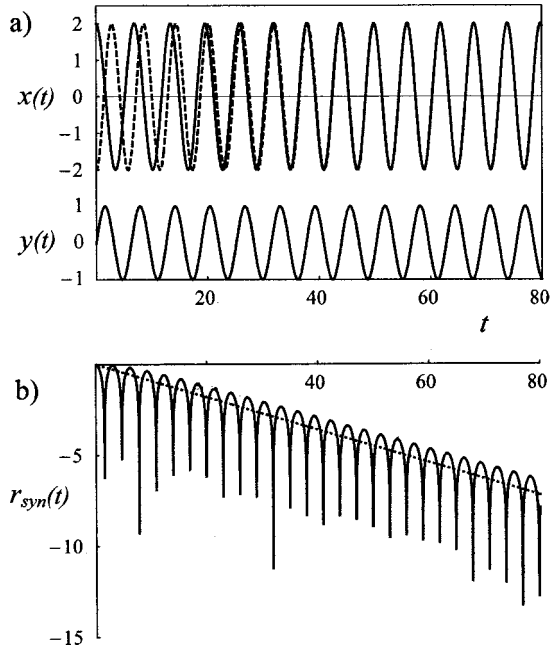

Fig. 3. (a) Plot of $x(t)=2\sin\theta(t)$ for two periodically driven phase oscillators described by Eq. (6) with $b=0.1$ and $\phi(t)=1.05t$. The driving force, $y(t)=\sin\phi(t)$, is shown in the lower curve. For the initial conditions, $x_1(0)=2$ (solid line) and $x_2(0)=-2$ (dashed line), the solutions converge to indistinguishable curves by $t=40$. (b) The rate of convergence is determined by the negative slope of $\langle r_{\rm syn}(t)\rangle\approx -0.09t$ indicated by the dotted line.

For example, Fig. 3(a) shows numerical results for the coupling of a periodic drive, $\phi(t)=\omega t$, with $\omega=1.05$ and $B=0.1$, to two phase oscillators with $\Omega=1$ and $b=0.1$. Starting from $\theta_1(0)=\pi/2$ and $\theta_2(0)=-\pi/2$, the solutions, $x_{1,2}(t)=\sin\theta_{1,2}(t)$, converge rapidly to synchronized, mode-locked behavior. The rate of asymptotic convergence can be determined from the negative average slope of $\langle r_c(t)\rangle\approx -0.09t$ in Fig. 3(b) and agrees with the analytical prediction of the Lyapunov exponent, $\gamma=0.09$, given by Eq. (13).

On the other hand, if ω is very different than Ω, or if the coupling is too weak [so that Eq. (7) is not satisfied], there is no asymptotic convergence to a common, mode-locked solution. The evolution of $x(t)$ is quasiperiodic and different initial conditions will generally lead to distinct long-time solutions so that there is no synchronization.

More specifically, the solution to Eq. (6) for small b is approximately $\theta(t)\approx\Omega t+\theta_0+O(b)$. In this case, Eq. (12) indicates that nearby solutions with $\delta(0)=\theta_1(0)-\theta_2(0)=\eta_1(0)-\eta_2(0)\ll 1$ will initially diverge or converge, depending on the initial phases and will subsequently oscillate quasiperiodically as

$$\delta(t)\approx\delta(0)e^{-b(\sin[(\Omega-\omega)t+\theta_0]-\sin\theta_0)/(\Omega-\omega)}. \tag{14}$$

Although the time-averaged Lyapunov exponent is zero, it is important to note that Eq. (14) indicates that for $|b|<|\Omega-\omega|$, the difference in phases of nearby solutions can nevertheless be amplified or diminished by a factor of $e^{\pm b/(\Omega-\omega)}\leqslant 2.72$.

The inequality in Eq. (7) defines a triangular stable zone, the so-called Arnold tongue, in the coupling-frequency parameter space (see Fig. 4). For b and ω inside this stable zone, the time-evolution of the driven phase oscillator is entrained to the periodic drive and converges asymptotically to a common phase-locked state at a rate determined by the Lyanpunov exponent given by Eq. (13), which is greatest when $\omega\approx\Omega$ and the coupling b is large, as indicated by the shading in Fig. 4. At the edge of the stable zone, the rate of convergence goes to zero and remains zero outside of the stable zone where the long-time behavior of $x(t)$ is quasiperiodic.

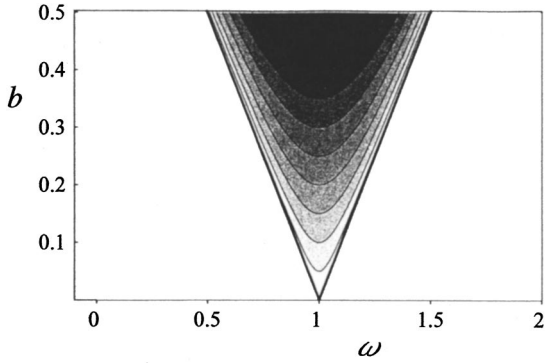

Fig. 4. The Arnold tongue in the $b-\omega$ plane. The boundary of the mode-locking region in the coupling-frequency parameter space is defined by Eq. (7). The grayscale contours indicate the increasing convergence rate, Eq. (13), from $\gamma=0$ (white) outside of the tongue to $\gamma=b=0.5$ (black) at the center-top.

Another important feature of the asymptotic stability and synchronization of periodically driven nonlinear oscillators is that this behavior persists even for small changes in the parameters of the oscillators. For example, as long as b, Ω, and ω lie within the stable zone prescribed by Eq. (7), small changes in these parameters cause only small shifts in the mode-locked phase η_∞. Consequently, the synchronization of periodically driven phase oscillators is structurally stable. If two different oscillators, x and $\tilde{x}$, with slightly different natural frequencies, $\Delta\Omega=\Omega-\tilde{\Omega}$, or coupling strengths, $\Delta b=b-\tilde{b}$, are driven by periodic forces with frequency ω well inside the respective stable zones defined by Eq. (7), both oscillators will still be entrained to the periodic drive and will be approximately synchronized with a small, constant phase difference,

$$\Delta\eta_\infty=\eta_\infty-\tilde{\eta}_\infty\approx\frac{1}{\gamma}\left[\Delta\Omega-(\Omega-\omega)\frac{\Delta b}{b}\right], \tag{15}$$

given by the leading terms in the Taylor expansion of Eq. (9).

This approximate synchronization breaks down only near the edge of the stable zone where $\gamma\to 0$. Outside the stable zone, the evolution of the two oscillators will be distinctly different due to differences in their initial conditions and parameters. Even if the two oscillators had the same initial conditions, they would continuously slip out of phase at a rate given approximately by $\Delta\Omega$.

III. PHASE MODEL WITH TIME-VARYING DRIVE FREQUENCY

To simplify the analysis of the response of the nonlinear phase oscillator to a time-varying drive, we start with the equation for $\eta(t)$. If $\omega(t)=\dot{\phi}$ is time-dependent, Eq. (8) generalizes to

$$\frac{d\eta}{dt}=[\Omega-\omega(t)]-b\sin\eta. \tag{16}$$

The previous analysis for constant frequency drive suggests that nearby solutions will tend to converge when $\omega(t)$ lies within the stable zone[9]

$$\left|\frac{\Omega-\omega(t)}{b}\right|<1. \tag{17}$$

In particular, if $\omega(t)$ changes slowly through the stable zone, then $\theta(t)$ will try to track $\phi(t)$, the phase of the drive. If the coupling is strong enough to ensure that the tracking is close, so that $|\eta(t)|<\pi/2$, then nearby solutions to Eq. (16) with small $\delta(t)=\theta_1(t)-\theta_2(t)=\eta_1(t)-\eta_2(t)$ will converge exponentially at the instantaneous rate, $\gamma(t)=b\cos[\eta(t)]>0$, because the linearization of Eq. (16) is also given by Eq. (12). On the other hand, when $\omega(t)$ is outside the stable zone and $\eta(t)$ is no longer constrained to be small, nearby solutions to Eq. (16) will alternately move apart or together depending on the sign of $\cos[\eta(t)]$.

To estimate the conditions on b and the rate of change of $\omega(t)$ for close tracking of the driving phase, the results for the constant frequency drive can be generalized by considering a solution to Eq. (16) of the following form:

$$\eta(t)=\arcsin\left[\frac{\Omega-\omega(t)}{b}\right]+\xi(t). \tag{18}$$

Convergence occurs when $|\arcsin[(\Omega-\omega)/b]+\xi|<\pi/2$. Because this condition is met as long as ω is in the stable zone, $|\Omega-\omega(t)|<|b|$, the stability depends crucially on the magnitude of $\xi(t)$.

If we substitute Eq. (18) into Eq. (16), we obtain an equation for $\xi(t)$:

$$\frac{d\xi}{dt}=\Omega-\omega(t)+\frac{d\omega(t)}{dt}\Big/\sqrt{b^2-(\Omega-\omega(t))^2}\\ -b\sin[\arcsin[(\Omega-\omega(t))/b]+\xi(t)]. \tag{19}$$

If $\xi\ll 1$, then Eq. (19) can be simplified to

$$\frac{d\xi}{dt}=\frac{d\omega(t)}{dt}\Big/\sqrt{b^2-(\Omega-\omega(t))^2}\\ -\sqrt{b^2-(\Omega-\omega(t))^2}\,\xi(t), \tag{20}$$

which converges to the approximate solution

$$\xi_\infty(t)\simeq\frac{d\omega(t)}{dt}\Big/[b^2-(\Omega-\omega(t)^2] \tag{21}$$

at the instantaneous rate,[9]

$$\gamma(t)=\sqrt{b^2-(\Omega-\omega(t))^2}+O(\xi). \tag{22}$$

The consistency of these approximate solutions and the assumptions used to derive them impose explicit (sufficiency) conditions for convergence on the magnitude of b and $\dot\omega$. In particular, for ξ_∞ to be small, b and $\dot\omega$ must satisfy the adiabaticity condition [see Eq. (21)]:[9]

$$R_A=\frac{1}{b^2}\dot\omega(t)\ll 1. \tag{23}$$

Because the width of the stable frequency zone is $2b$, an estimate of the transit time of $\omega(t)$ through the stable zone is $T=2b/\dot\omega(t)$. The adiabaticity condition, Eq. (23), corresponds to the requirement that the convergence time, $1/\gamma\approx 1/b$, be small in comparison to the transit time T.

When the adiabaticity condition is met, two nearby solutions will converge toward synchronization as they approach the common asymptotic solution,

$$\theta(t)=\phi(t)+\arcsin[(\Omega-\omega(t))/b]+\xi_\infty(t), \tag{24}$$

during the transit through the stable zone defined by Eq. (17). In particular, if we neglect small corrections to Eq. (22) of $O(\xi)$, nearby solutions can be expected to converge by an exponential factor of

$$\exp\left(-\int_{t_0}^{t_f}\gamma(t)dt\right)\approx\exp\left(-\int_{t_0}^{t_f}\sqrt{b^2-(\Omega-\omega(t))^2}\,dt\right) \tag{25}$$

between t_0 when $\omega(t)$ enters the stable zone and t_f when it leaves.

When $\omega(t)$ leaves the stable zone, $\theta(t)$ is no longer constrained to closely track $\phi(t)$, with $|\eta(t)|<\pi/2$, and when $\cos[\eta(t)]<0$, nearby solutions will move apart. Consequently, two driven oscillators will desynchronize whenever $\omega(t)$ leaves the stable zone. [Note that the oscillators may briefly continue to synchronize for driving frequencies outside the stable zone as long as $|\eta(t)|<\pi/2$.] Nevertheless, synchronization will be restored when the drive frequency enters the stable zone again as long as T is much bigger than $1/\gamma(t)$.

As in the constant frequency case, this synchronization will be structurally stable in the sense that the evolution of two oscillators, $x(t)$ and $\tilde x(t)$, with small differences, $\Delta\Omega$ and Δb, will approximately synchronize with a small (bounded) phase difference,[9]

$$\Delta\eta=\eta-\tilde\eta\approx[\Delta\Omega-(\Omega-\omega(t))(\Delta b/b)]/\gamma(t)+O(\xi). \tag{26}$$

In addition, the approximate stabilization will be robust to small (bounded) differences in the driving phase, $\Delta\phi(t)=\phi(t)-\tilde\phi(t)$, and driving frequency, $\Delta\omega(t)=\omega(t)-\tilde\omega(t)$, because Eq. (24) shows that

$$\theta(t)-\tilde\theta(t)=\Delta\phi(t)-\Delta\omega(t)/\gamma(t)+O(\xi). \tag{27}$$

In Secs. III A and III B this theory is used to predict the conditions for asymptotic stability and the rates of synchronization for a linearly changing and randomly varying drive frequency. (The theory is applied to the intermediate case of a parabolically varying drive frequency in Appendix A.) In the linear case all of the estimates can be performed analytically. In the random case the ergodic theorem can be used to convert the time-integral of the convergence rate in Eq. (25) to an ensemble average over the random drive. In both cases the theoretical predictions are compared with numerical results.

A. Linear frequency change: $\omega(t)=\Omega+mt$

If $\omega(t)=\dot\phi$ varies linearly in time, $\omega(t)=\Omega+mt$, then nearby solutions to Eq. (16) will converge during the time that $\omega(t)$ is within the stable zone, Eq. (17), from $t_0=-b/m$ to $t_f=+b/m$, as long as the change in drive frequency is sufficiently slow. In this case the solution to Eq. (16) is

$$\eta(t) = \arcsin[-mt/b] + \xi(t), \tag{28}$$

where Eq. (21) gives an approximate expression for

$$\xi_\infty(t) \simeq \frac{m}{b^2 - m^2 t^2}, \tag{29}$$

which is small near the center of the stable zone (for $t \approx 0$) if

$$m/b^2 \ll 1. \tag{30}$$

The instantaneous convergence rate in the stable zone, Eq. (22), is approximately

$$\gamma(t) \simeq \sqrt{b^2 - m^2 t^2} + \frac{mt}{b}\,\xi_\infty(t). \tag{31}$$

When integrated over the transit time through the stable zone from t_0 to t_f, the small (odd) contributions of $t\xi(t)$ are neglected to yield an average convergence rate,

$$\Gamma \approx \frac{1}{T}\int_{-b/m}^{b/m} \sqrt{b^2 - m^2 t^2}\, dt = \frac{\pi b^2}{2mT} = \frac{\pi b}{4}. \tag{32}$$

Consequently, two nearby solutions will converge by a factor of $e^{-\pi b^2/2m}$ during the transit time $T = 2b/m$ through the stable zone. The requirement that ξ_∞ be small, $m/b^2 \ll 1$, directly corresponds (to a numerical factor of $2/\pi$) to the adiabaticity condition, Eq. (23), which is that the average convergence time, $1/\Gamma$, be small in comparison to T.

These theoretical predictions are compared in Fig. 5 with the numerical solutions of the driven phase model, Eq. (16), for $b = 0.5$ and $\Omega = 1$. The phase is $\phi(t) = t^2/80$ corresponding to $m = 1/40$. The drive frequency starts at $\omega(0) = 0$ and first enters the stable zone defined by Eq. (17) when $t = 20$. Figure 5(a) shows that two oscillators with different initial conditions rapidly synchronize when the drive frequency enters the stable zone. The instantaneous convergence rate of the numerical solutions can be estimated from the slope of $r_{\rm syn}(t)$ shown in Fig. 5(b). As expected, the average slope is approximately zero until $t = 20$, is negative (indicating the convergence of the two solutions) during the transit through the stable zone, and returns to zero outside the stable zone for $t > 60$. After the linear transit through the stable zone for time $T = 2b/m = 40$, the average distance between the phases of the two oscillators is reduced by a factor of approximately e^{-16}, which is in good agreement with the theoretical prediction of $e^{-\pi b^2/2m} = e^{-5\pi}$ given by Eq. (32).

When $\omega(t)$ passes slowly through the stable zone, the phases of the two driven oscillators, $\theta_{1,2}(t)$, synchronize as they try to track the driving phase $\phi(t)$. The phase-locking is not perfect as in the constant frequency case. Nevertheless, Fig. 5(c) shows that inside the stable zone from $t = 20$ to 60, the phase difference $\eta(t) = \theta(t) - \phi(t) \pmod{2\pi}$ is relatively small and agrees very well with the theoretical prediction, Eq. (28), with $\xi_\infty(t)$ defined by Eq. (29).

In the example displayed in Fig. 5, the instantaneous convergence time at the center of the stable zone at $T = 40$ is estimated from Eq. (22) to be $1/\gamma(40) \approx 2$. Because this convergence time is much shorter than the transit time $T = 20$ through the stable zone, the adiabaticity condition, Eq. (23), with $R_A = 1/10$ is well satisfied. In fact, the time for exponential convergence is even short compared with the natural period of oscillation, $\tau = 2\pi$, so that nonlinear oscillators can converge significantly in one period as indicated in Fig. 5(a). As expected, the adiabatic theory only breaks down near the edges of the stable zone at $t = 20$ and at $t = 60$ [see Fig. 5(c)]. However, when the adiabaticity condition is not satisfied and the transit time through the stable zone is short compared to the convergence time, the numerical solutions indicate that any small tendency for two nearby oscillators to synchronize during this brief transit time is often overcome by the divergence of the solutions, described by Eq. (14), when the drive frequency exits the stable zone.

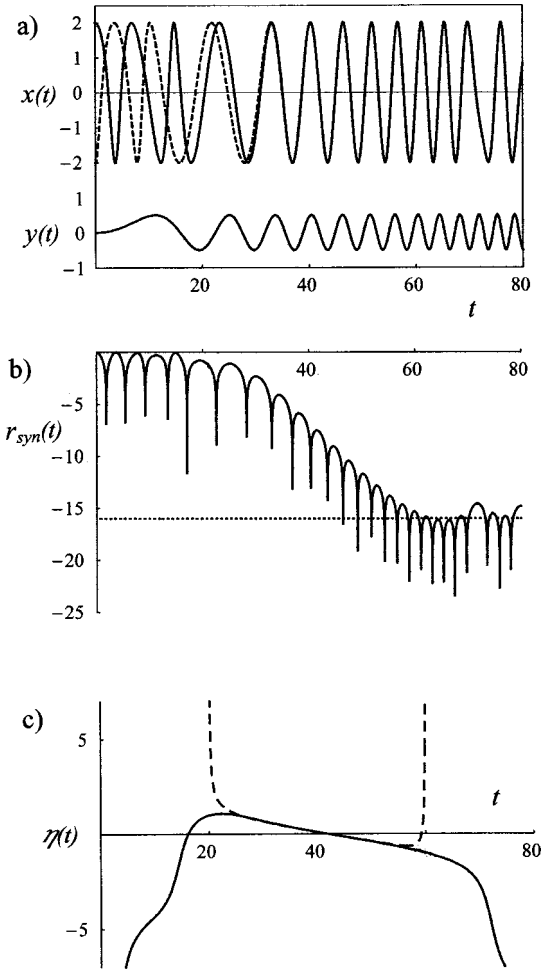

Fig. 5. (a) Plot of $x(t) = 2\sin\theta(t)$ for two driven phase oscillators described by Eq. (16) with $b = 0.5$, $\Omega = 1$, and $\phi(t) = t^2/80$. The driving force, $y(t) = \sin\phi(t)$, with linearly varying frequency, $\omega(t) = t/40$, is shown in the lower curve. For the initial conditions, $x_1(0) = 2$ (solid line) and $x_2(0) = -2$ (dashed line), the two solutions show no sign of convergence until $\omega(t)$ enters the stable zone at $t = 20$. (b) The instantaneous rate of convergence from $r_{\rm syn}(t)$. After passage through the stable zone, the total convergence factor is $\approx e^{-16}$ as indicated by the dotted line. (c) The difference between $\theta(t)$ and $\phi(t) \pmod{2\pi}$ as a function of time (solid curve) shows that the phase of the driven oscillator only tends to track the driving phase when $\omega(t)$ is in the stable zone between $t = 20$ and 60. Even in the stable zone, the phases are not perfectly locked, but the difference, $\eta(t)$, is very well described inside the stable zone by the correction (28) with $\xi_\infty(t)$ defined by Eq. (29) (dashed curve).

B. Random drive: $\phi(t) = \phi_r(t)$

Not surprisingly, if we drive the phase of oscillator x with a randomly varying phase, $\phi_r(t)$ in Eq. (6), then $\theta(t)$ and

$x(t)$ will also exhibit random fluctuations. It is remarkable, however, that the evolution may nevertheless be asymptotically stable so that two oscillators, x_1 and x_2, starting from different initial conditions, will still synchronize to the same randomly fluctuating behavior.[9] In addition, this asymptotic stability is structurally stable in the sense that the (near) synchronization of two randomly driven oscillators persists for small differences in Ω and b and even for small differences in additional noise in the fluctuating phase $\phi_r(t)$.[9]

If we define the randomly fluctuating drive frequency, $\omega_r(t)=\dot{\phi}_r(t)$, we can apply the previous results for the time-varying drive frequency to determine approximate conditions for asymptotic stability for the solutions to

$$\frac{d\eta}{dt}=[\Omega-\omega_r(t)]-b\sin\eta. \tag{33}$$

In particular, two nearby oscillators will synchronize when the drive frequency passes slowly through the stable zone defined by Eq. (17) and the instantaneous convergence rate will be approximately determined by

$$\gamma(t)=\begin{cases}\sqrt{[b^2-(\Omega-\omega_r(t))^2}, & \text{for } |\Omega-\omega_r(t)|<|b|\\ 0, & \text{for } |\Omega-\omega_r(t)|\geqslant|b|\end{cases}. \tag{34}$$

The time-averaged convergence rate will be determined by

$$\Gamma=\frac{1}{T}\int_0^T\gamma(t)dt. \tag{35}$$

An example of the synchronization of randomly driven phase oscillators described by Eq. (33) with $\Omega=1$ and $b=0.5$ is illustrated in Fig. 6. Starting from the initial conditions, $\theta_1(0)=\pi/2$ and $\theta_2(0)=-\pi/2$, the two phase oscillators, $x_{1,2}(t)=2\sin\theta_{1,2}(t)$, shown in Fig. 6(a) (top), are coupled to the same driving oscillator, $y(t)=\sin\phi_r(t)$, shown in Fig. 6(a) (bottom), with a randomly varying phase, $\phi_r(t)$, corresponding to a low-pass filtered, Gaussian random process.[20] Although $x_{1,2}(t)$ exhibit irregular fluctuations in response to the randomly varying phase, $\phi_r(t)$, they nevertheless synchronize to indistinguishable trajectories by $t=40$. The asymptotic stability is illustrated by the average negative slope of $r_{\rm syn}(t)$ [see Fig. 6(b)], which arises from multiple passes of the fluctuating $\omega_r(t)$ through the stable zone shown in Fig. 6(c).

Because $\phi_r(t)$ and $\omega_r(t)$ are both random functions, the description of the synchronization of randomly driven phase oscillators can be simplified using the ergodic theorem[20] to express the time-average of the convergence rate in Eq. (35) in terms of the ensemble average,

$$\Gamma=\int_{\Omega-b}^{\Omega+b}\sqrt{b^2-(\Omega-\omega_r)^2}P(\omega_r)d\omega_r, \tag{36}$$

where $P(\omega_r)$ is the probability distribution for the randomly fluctuating drive frequency. In particular, if $\phi_r(t)$ is a low-pass filtered, Gaussian random process with a power spectrum $S(f)$ and distribution,

$$P(\phi_r)=\frac{1}{\sqrt{2\pi\sigma}}e^{-\phi_r^2/2\sigma}, \tag{37}$$

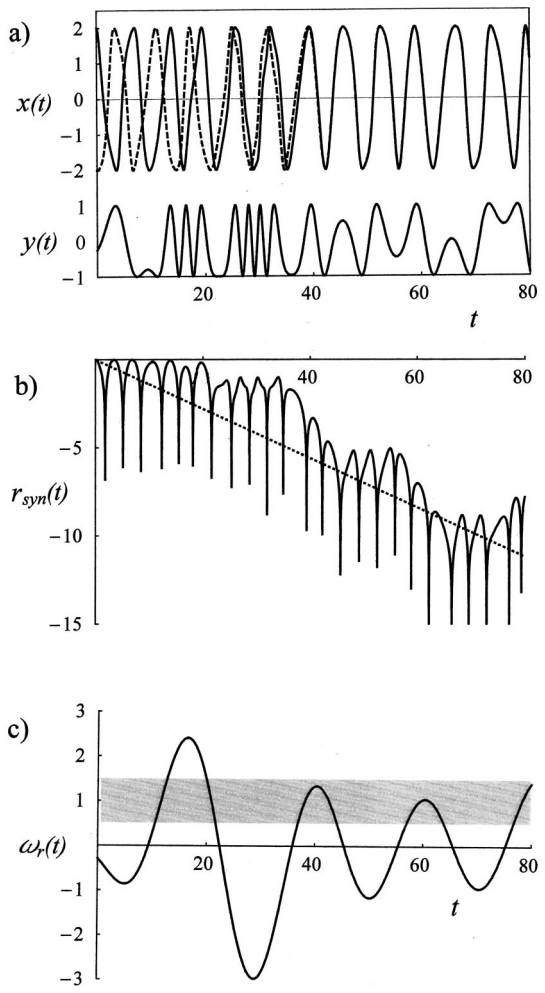

Fig. 6. (a) Plot of $x(t)=2\sin\theta(t)$ for two randomly driven phase oscillators described by Eq. (33) with $\Omega=1$ and $b=0.5$ driven by a low-pass filtered Gaussian random phase, $\phi_r(t)$, with variance $\sigma\simeq30$, $\sigma_\omega=1$, and $\sqrt{\sigma_{\omega'}}\simeq0.24$. The driving force, $y(t)=\sin\phi_r(t)$, is shown in the lower curve. For initial conditions, $x_1(0)=2$ (solid line) and $x_2(0)=-2$ (dashed line), the solutions converge to indistinguishable curves by $t=40$. (b) The mean rate of convergence from $\langle r_{\rm syn}(t)\rangle\simeq-0.14t$ is indicated by the dotted line. (c) The randomly fluctuating frequency $\omega_r(t)$ driving both oscillators is shown crossing in and out of the stable frequency zone shaded in gray. Note that the times of large average negative slope in (b) correspond to the times when $\omega_r(t)$ is passing through the stable zone.

with variance $\sigma=\int_0^\infty S(f)df$, then the probability distribution for ω_r is also Gaussian,[20]

$$P(\omega_r)=\frac{1}{\sqrt{2\pi\sigma_\omega}}e^{-\omega_r^2/2\sigma_\omega}, \tag{38}$$

with variance $\sigma_\omega=\int_0^\infty f^2S(f)df$.

Consider, for example, the randomly fluctuating driving phase represented by the Fourier series,

$$\phi_r(t)=\sum_{n=1}^{N}a_n\sin(f_nt+\zeta_n), \tag{39}$$

with frequencies $f_n=2\pi n/\tau$, uniform amplitudes $a_n=\sqrt{2\sigma/N}$, and ζ_n randomly distributed over the interval $[0,2\pi]$. In the large N limit, ϕ_r has a Gaussian distribution

with variance σ and the driving frequencies have a Gaussian distribution with variance,[21]

$$\sigma_\omega = \frac{\sigma}{N}\sum_{n=1}^{N} f_n^2 = \left(\frac{2\pi}{\tau}\right)^2 \sigma(N+1)(2N+1)/6 \approx \sigma f_N^2/3, \tag{40}$$

where f_N is the highest frequency in Eq. (39). For finite N, Eq. (39) provides a very convenient approximation of a low-pass filtered, Gaussian random process, with σ_ω given by Eq. (40).

The combination of the results of Eqs. (36) and (38) provides a useful estimate for the average convergence rate for the randomly driven oscillator. In particular, when the stable zone is very narrow, $b \ll \Omega$, the integral in Eq. (36) can be further approximated by assuming that $P(\omega_r)$ does not vary much over the stable zone. Then the average convergence rate is simply given by[9]

$$\Gamma \approx \frac{\pi b^2}{2}\frac{1}{\sqrt{2\pi\sigma_\omega}} e^{-\Omega^2/2\sigma_\omega}. \tag{41}$$

This simple estimate predicts an average convergence rate of $\Gamma = 0.095$ for the two randomly driven phase oscillators in Fig. 6 with $b = 0.5$ and $\sigma_\omega = 1$, which is in reasonable agreement with the numerical value of $\Gamma \approx 0.14$ seen in Fig. 6(b) for the particular realization of the random drive shown in Fig. 6(c).

For Gaussian random phase drives, the adiabaticity condition for synchronization, Eq. (23), can be roughly estimated using the variance of the derivative of the drive frequency, $\sigma_{\omega'} = \int_0^\infty f^4 S(f)\, df$. In particular, for the random phases defined by Eq. (37),

$$\sigma_{\omega'} = \sigma\left(\frac{2\pi}{\tau}\right)^4 (N+1)(2N+1)(3N^2+3N-1)/30 \approx \tfrac{3}{5}\sigma_\omega f_N^2. \tag{42}$$

An adiabaticity condition[9] for the random phase drive can be expressed by the requirement that

$$\overline{R_A} = \sqrt{\sigma_{\omega'}}/b^2 \ll 1. \tag{43}$$

Because the Gaussian distribution of ω' is peaked around zero, this rough estimate of the ratio of the rate of change of the fluctuating ω to the convergence rate based on the rms value of ω' is very conservative. For example, in Fig. 6 the driven phase oscillators with $b = 0.5$ and $\sqrt{\sigma_{\omega'}} = 0.24$ exhibit strong synchronization even though $\overline{R_A} \simeq 1$.

In Fig. 7, the numerically calculated convergence rates averaged over a large number of realizations of the random drive, Eq. (39), are compared with the approximate convergence rates predicted by Eq. (41). When $\overline{R_A}$ is small, the measured rates of synchronization are in good agreement with the simple theoretical prediction, Eq. (41). Both the measured results and the theoretical predictions are small when σ_ω is small, because ω_r rarely enters the primary stable zone near $\omega = 1$ (see Fig. 4). The convergence rates peak around $\sigma_\omega = 1$ and then decline slowly for larger values of σ_ω because the frequency of the random drive has a higher probability of leaving the primary stable zone again. However, when $\overline{R_A}$ is large and ω_r passes rapidly through the stable zone of the periodically driven oscillator, the synchronization rates are greatly reduced. In Figs. 6 and 7 the randomly varying phase $\phi_r(t)$ was generated using Eq. (39) with $\tau = 200$. The low-pass filtered random phase used in Fig. 6 and the small $\overline{R_A}$ simulations in Fig. 7 used only $N = 10$ Fourier components. (The large $\overline{R_A}$ simulations in Fig. 7 used $N = 100$ Fourier components.) In every case the value of σ was adjusted so that Eq. (40) gave the desired value of σ_ω. One drawback of this construction of the random phase is that $\sigma_{\omega'}$ and $\overline{R_A}$ also increase with σ_ω, as indicated in Eq. (42), which may account for the larger discrepancies between the theoretical predictions for the synchronization rates and the simulations in Fig. 7 for large σ_ω.

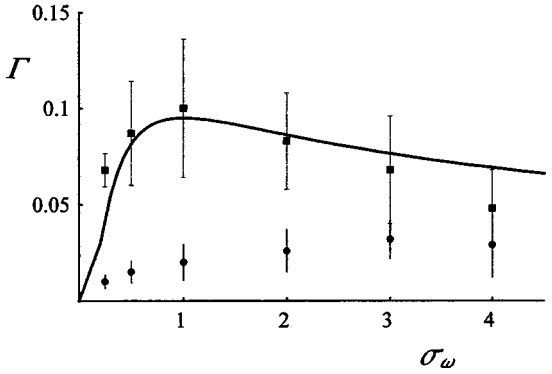

Fig. 7. The synchronization rates, Γ, predicted by Eq. (41) for randomly driven phase oscillators with $\Omega = 1$ and $b = 0.5$ (solid curve) are compared with the results of numerical simulations as a function of σ_ω for small values of the adiabaticity parameter (squares) with $\overline{R_A}$ between 0.5 and 2 (plotted from left to right) and for large $\overline{R_A} = 5-20$ (dots). The synchronization rates in the simulations were determined from $\langle r_{\rm syn}(t)\rangle$ for two identical driven oscillators with different initial conditions. The average data and error bars were computed using five different realizations of the random drive for each σ_ω.

IV. AN ILLUSTRATIVE EXAMPLE: THE VAN DER POL OSCILLATOR

The equation of motion of the van der Pol oscillator was given in Eq. (2) [with $F(t) = 0$] and leads to a stable, self-sustained limit cycle. We rewrite this second-order differential equation as a pair of first-order equations for position and velocity,

$$\frac{dx}{dt} = v, \tag{44a}$$

$$\frac{dv}{dt} = \epsilon(1-x^2)v - \Omega^2 x, \tag{44b}$$

and look for oscillatory solutions of the following form:[22,23]

$$x(t) = a(t)\sin\theta(t), \tag{45a}$$

$$v(t) = \Omega a(t)\cos[\theta(t)]. \tag{45b}$$

The equivalent system of differential equations for the amplitude $a(t)$ and the phase $\theta(t)$ are

$$\frac{dx}{dt} = \dot{a}\sin\theta + a\dot{\theta}\cos\theta = \Omega a\cos\theta, \tag{46a}$$

$$\frac{dv}{dt} = \Omega \dot{a} \cos\theta - \Omega a \dot{\theta} \sin\theta$$

$$= \epsilon(1 - a^2 \sin^2\theta)\Omega a \cos\theta - a\Omega^2 \sin\theta. \tag{46b}$$

These equations can be simplified further by multiplying Eq. (46a) by $\Omega \sin\theta$ and Eq. (46b) by $\cos\theta$ and taking the sum to obtain a first-order differential equation for the amplitude,

$$\dot{a} = \epsilon(1 - a^2 \sin^2\theta) a \cos^2\theta. \tag{47}$$

Similarly, if we multiply Eq. (46a) by $\Omega \cos\theta$ and Eq. (46b) by $\sin\theta$ and take the difference, we obtain an equation for the phase

$$\dot{\theta} = \Omega - \epsilon(1 - a^2 \sin^2\theta)\cos\theta \sin\theta. \tag{48}$$

For small ϵ the rapidly varying terms with $\sin\theta\cos\theta = \sin 2\theta/2$ may be neglected and $\cos^2\theta$ and $\sin^2\theta\cos^2\theta$ may be approximated by their averages 1/2 and 1/8, respectively. Then the approximate equations for the amplitude and phase of the van der Pol oscillator reduce to the familiar forms,[3,5]

$$\frac{da}{dt} \approx \frac{\epsilon a}{2}(1 - a^2/4), \tag{49a}$$

$$\frac{d\theta}{dt} \approx \Omega. \tag{49b}$$

Equation (49) predicts that every solution converges to the self-sustained limit cycle $x(t) \approx 2\sin[\theta(t)]$ with $\theta(t) \approx \Omega t + \theta(0)$.

The same analysis can be repeated for the driven van der Pol oscillator. In this case the exact equations for the amplitude and phase, Eqs. (47) and (48), are simply modified by the addition of terms involving the driving force, $F(t)$,

$$\dot{a} = \epsilon(1 - a^2 \sin^2\theta) a \cos^2\theta + F(t)\cos\theta/\Omega, \tag{50a}$$

$$\dot{\theta} = \Omega^2 - \epsilon(1 - a^2 \sin^2\theta)\cos\theta \sin\theta - F(t)\sin\theta/a\Omega. \tag{50b}$$

In particular, if we couple one van der Pol oscillator, $x(t)$, to a second oscillator, $y(t) = B\sin\phi(t)$, or simply choose $F(t)$ to have this form, the driving terms in Eqs. (47) and (48) are $B\sin\phi\cos\theta/\Omega$ and $-B\sin\phi\sin\theta/a\Omega$, respectively. Again for small ϵ, Eq. (50) can be approximated by neglecting rapidly oscillating terms. If we take $\langle\cos^2\theta\rangle = 1/2$ and $\langle\sin^2\theta\cos^2\theta\rangle = 1/8$, we obtain

$$\frac{da}{dt} \approx \frac{\epsilon a}{2}(1 - a^2/4) + B\sin\phi\cos\theta/\Omega, \tag{51a}$$

$$\frac{d\theta}{dt} \approx \Omega - \frac{B}{a(t)\Omega}\sin\phi\sin\theta. \tag{51b}$$

Moreover, for weak coupling, $B \ll 1$, we can still approximate the solution to the amplitude equation, Eq. (51a), by $a(t) \approx 2$, so that the approximate description of the driven van der Pol equation can be reduced to the phase equation alone,

$$\frac{d\theta}{dt} \approx \Omega - \frac{B}{2\Omega}\sin\phi\sin\theta, \tag{52}$$

which is equivalent to the phase model,[9]

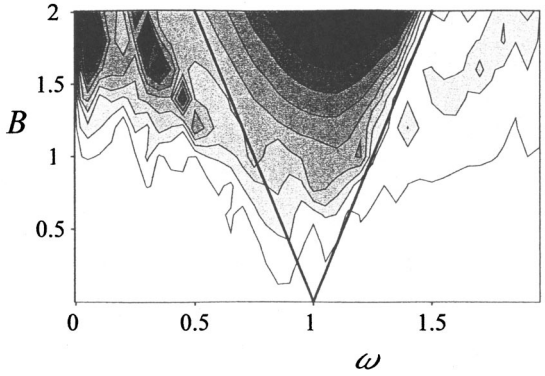

Fig. 8. The Arnold tongues in the $B-\omega$ plane describe the stable zones for asymptotic stability for the periodically driven van der Pol oscillator with $\epsilon = 1$. The grayscale contours indicate the numerically calculated rates of exponential convergence ranging from 0 (white) to ≈ 0.5 (black). The boundary of the stable zone predicted by the phase model, corresponding to Fig. 4 with $b = B/4$, is indicated by the solid line.

$$\frac{d\theta}{dt} = \Omega - \frac{B}{4\Omega}[\cos(\theta - \phi) - \cos(\theta + \phi)]. \tag{53}$$

When the driving term has a constant frequency ω, we can approximate Eq. (53) further by neglecting the rapidly oscillating term $\cos(\theta + \omega t)$ to arrive at the simple phase model (shifted by $\pi/2$) studied previously:

$$\frac{d\theta}{dt} \approx \Omega - b\cos(\theta - \omega t), \tag{54}$$

with $b = B/4\Omega$. The analytical results for the asymptotic stability of the phase model with constant ω provide a simple derivation of the extent of the primary stable zone for the van der Pol oscillator. In particular, Eq. (7) predicts mode-locked behavior for

$$\frac{B}{4\Omega} > |\Omega - \omega|. \tag{55}$$

This result can be compared with the more elegant, but much more complicated analysis found in standard treatments (see Appendix B).[4–6,22] In particular, for the van der Pol oscillators considered in Fig. 1 with $\epsilon = 1$, $\Omega = 1$, $B = 0.5$, and $\omega = 1.05$, the analysis for the constant phase model, Eq. (55), predicts the observed asymptotic stability because $B/4\Omega = 0.125 > |\Omega - \omega| = 0.05$. The phase model also predicts the convergence rate, Eq. (13), with $\gamma = 0.115$, which agrees reasonably well with 0.08, the average negative slope of $r_{\text{syn}}(t)$ [see Fig. 1(b)].

In fact, for $\epsilon = 1$ the Arnold tongues in the $B-\omega$ parameter space for the driven van der Pol oscillator shown in Fig. 8 are well approximated by the stable zone for the simple phase model shown in Fig. 4. The key differences are that the van der Pol oscillator has multiple stable zones at some rational multiples (for example, 1/3, 1/2, 2, 3) of the natural frequency $\approx \Omega$ as well as for negative frequencies as indicated in Eq. (53). Nevertheless, Fig. 8 shows that the $B-\omega$ parameter space is dominated by a triangular stable zone for $\omega \simeq \Omega = 1$ (with a mirror image around $\omega \simeq -1$), which suggests that the previous results for the conditions for asymptotic stability and the rates of synchronization devel-

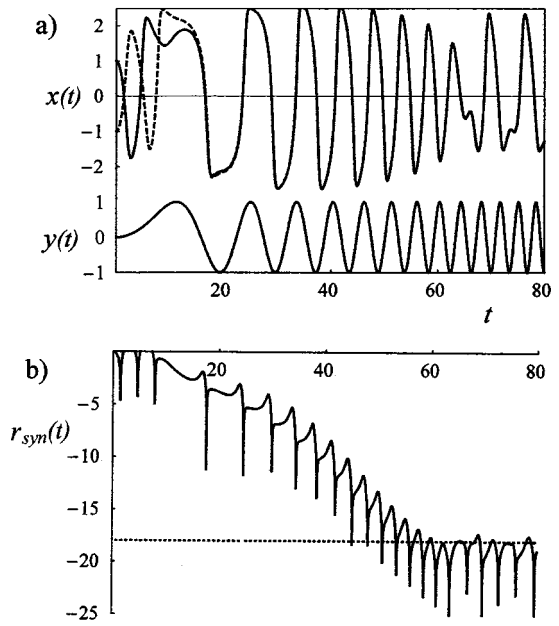

Fig. 9. (a) Plot of $x(t)$ for two driven van der Pol oscillators with $\epsilon=1$, $\Omega=1$, and an aperiodic drive, $F(t)=2\sin\phi(t)$ with $\phi(t)=t^2/80$, corresponding to the linearly varying drive frequency, $\omega(t)=t/40$, shown in the lower curve. For the initial conditions, $x_1(0)=1$ (solid line) and $x_2(0)=-1$ (dashed line), the two solutions show strong convergence when $\omega(t)$ enters the primary stable zone at $t=20$. (b) The instantaneous rate of convergence determined from $r_{\rm syn}(t)$, which is small for $t<20$, large for $20<t<60$, and zero for $t>60$ when $\omega(t)$ leaves the primary stable zone. The total convergence factor e^{-18} is indicated by the dotted line.

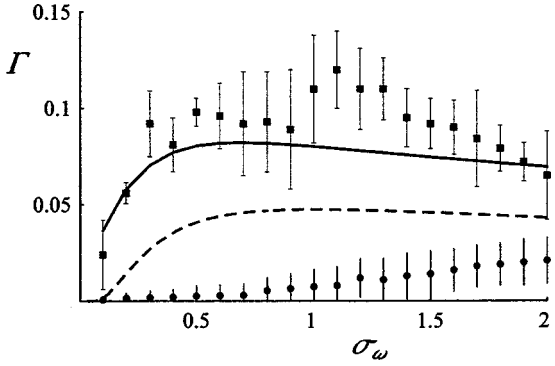

Fig. 10. The average synchronization rates, Γ, predicted by Eq. (56) for randomly driven van der Pol oscillators with $\epsilon=1$, $\Omega=1$, and $B=1.0$ (dashed curve), are compared with the results of simulations as a function of the variance in the drive frequency, σ_ω, for small values of the adiabaticity parameter (squares) with $\overline{R}_A$ between 0.5 and 2 (plotted from left to right) and for large $\overline{R}_A=5-20$ (dots). The synchronization rates were determined in the usual way. The average data and error bars were computed using five different realizations of the random drive for each σ_ω. The solid curve is a theoretical estimate of the convergence rates based on an average over the Arnold tongue rates calculated for periodically driven van der Pol oscillators.

oped for the phase model may be applied directly to the van der Pol oscillator, even with nonlinearity as large as $\epsilon=1$.

For example, Fig. 9 shows the synchronization of two van der Pol oscillators driven by the same linearly varying drive frequency, $\omega(t)=t/40$, used to synchronize the phase models in Fig. 5. In this case $B=2$ corresponds to the same coupling, $b=0.5$, used in Fig. 5. As in the phase model, Fig. 9(b) shows that $r_{\rm syn}(t)$ has an average negative slope for $20\leqslant t\leqslant 60$ when $\omega(t)$ is within the primary stable zone shown in Fig. 8. The total convergence factor, e^{-18}, at the end of the linear transit from $t=0$ to $t=80$ is somewhat smaller than for the phase model because of the additional stable zones near the 1/2 and 1/3 subharmonics indicated in Fig. 8, which cause the van der Pol oscillators to begin to converge before $t=20$ [see Fig. 9(b)].

Moreover, for a driving force with a randomly varying phase, $F_r(t)=B\sin\phi_r(t)$, we can use the correspondence with $b=B/4\Omega$ in the randomly driven phase model, Eq. (41), to estimate

$$\Gamma\approx\frac{e^{-\Omega^2/2\sigma_\omega}}{\sqrt{2\pi\sigma_\omega}}\,\frac{\pi B^2}{16\Omega^2} \tag{56}$$

for the average rate of synchronization for the weakly nonlinear van der Pol oscillator that is weakly driven by random phase. [Because both the positive and negative drive frequencies in Eq. (53) contribute to the convergence of the van der Pol oscillator to the synchronous solution, this estimate for the convergence rate is a factor of 2 larger than Eq. (41) for the phase oscillator with a single stable zone for positive frequencies alone.]

Although the synchronizing van der Pol oscillators with $\epsilon=1$ in Fig. 2 are not weakly nonlinear, the analytical relations from the phase model can still be used to provide rough estimates, within a factor of 2, for the adiabaticity conditions and rates for synchronization. For example, in Fig. 2 the two van der Pol oscillators with $\epsilon=1$ and $\Omega=1$ are synchronized by a random force with $B=1.0$ and $\sigma_\omega=1$ at an average exponential rate of $\Gamma\simeq 0.07$. In this case the adiabaticity parameter for the low pass filtered random phase is $\overline{R}_A\simeq 3.6$ [the low pass filter in Eq. (39) for this case was set by $N=20$]. Nevertheless, the convergence rate is still within a factor of 2 of the rate predicted by Eq. (56), that is, $\Gamma=0.05$.

Figure 10 shows a detailed comparison between the simple analytical estimate, Eq. (56), and the results of a large number of numerical simulations of van der Pol oscillators, with $\epsilon=1$, $\Omega=1$, and $B=1$, driven by different realizations of ϕ_r with σ_ω between 0 and 2. As long as $\overline{R}_A$ is small, the estimate of the convergence rate (dashed curve) based on the phase model is within a factor of 2 of the measured convergence rates. Both the numerical results and the theoretical predictions are small when σ_ω is small, because ω_r rarely enters the primary stable zone in Fig. 8 around $\omega=1$. The convergence rates peak around $\sigma_\omega=1$ and then decline slowly for larger values of σ_ω, because ω_r has a higher probability of passing out of the primary stable zone again. However, when $\overline{R}_A$ is large and ω_r passes rapidly through the primary stable zone in Fig. 8, the synchronization rates are greatly reduced.

Because the van der Pol oscillator admits additional stable zones near harmonic and subharmonics of the natural frequency of the nondriven oscillator, the phase model tends to underestimate the synchronization rate for variable frequency drives. In addition, the wider stable zones also prolong the transit times so that the phase model estimate for the adiabaticity parameter in Eq. (43) is excessively stringent. However, the general success of this adiabatic analysis suggests a

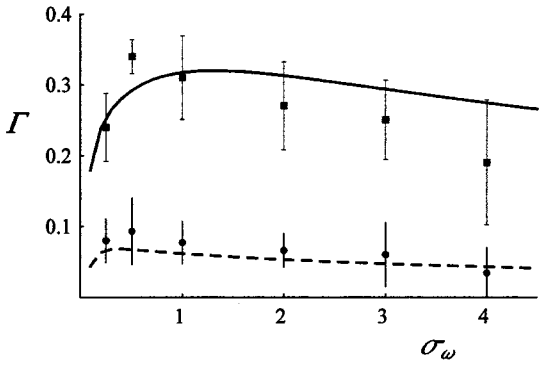

Fig. 11. The predicted synchronization rates, Γ, for randomly driven van der Pol oscillators with $\epsilon=4$, evaluated using the numerical results for periodic driving alone (curves), are compared with the results of simulations (dots) as functions of σ_ω for a strong driving force with $B=2$ (solid curve and small dots) and $B=1$ (dashed curve and large dots). (The mean and standard deviations were computed by averaging over five realizations of the random phase drive.) Remarkably, the adiabatic estimates show good agreement even though the approximate adiabaticity parameter for the random phase drive varies from $\overline{R_A}=1$ to 16 in these simulations.

practical procedure for assessing the asymptotic stability for strongly nonlinear oscillators when the reduction to the simple phase model breaks down. In these cases the synchronization rate can still be estimated for slowly varying frequency drives by first measuring the convergence rates for an array of constant drive frequencies spanning the Arnold tongues in the $B-\omega$ parameter space and then averaging over the statistical distribution of randomly varying drive frequencies, ω_r. In Fig. 10 the solid curve indicates the results of simply averaging the convergence rates for a cut through the stable zones in Fig. 8 at constant $B=1$ over Gaussian distributions of the drive frequencies, Eq. (38), with σ_ω between 0 and 2. Because this calculation includes the additional contributions of stable zones associated with subharmonics and higher harmonics of the natural oscillator frequency, it provides a much more accurate description of the measured synchronization rates.

The success of this practical program for characterizing the synchronization of randomly driven oscillators is further demonstrated in Fig. 11 for a strongly nonlinear van der Pol oscillator with $\epsilon=4$ that is strongly driven by randomly varying frequencies. In this case the stable zones for periodic drives, illustrated in the famous Fig. 12.12 from Hayashi,[4] differ in number and location from the phase model. (The strong nonlinearity significantly reduces the natural frequency of the van der Pol oscillator below $\Omega=1$.) Nevertheless, averages over the measured convergence rates give very good predictions for the convergence rates for strong coupling to randomly varying phase drives with $B=2$ and $B=1$. Remarkably, the theoretical estimates based on this adiabatic theory remain reasonably accurate even though the average adiabaticity parameter varied from $\overline{R_A}\simeq 1$ (for $\sigma_\omega=0.25$) to a high of $\simeq 16$ (for $\sigma_\omega=4$) in these simulations.

Finally, we note that, like the phase model, the asymptotic stability of the randomly driven van der Pol oscillator is structurally stable. As long as the adiabaticity criterion is satisfied so that the effective frequency of the drive, $\omega_r(t)$, passes slowly through the stable zones, then two slightly different nonlinear oscillators (even with slightly different random drives) will synchronize with at most a small phase shift. In fact, the structural stability is remarkably robust. Even if Ω, B, or the phase of the random drive, ϕ_r, for one of the van der Pol oscillators in Fig. 2 is changed by a few percent, the synchronization displayed in Fig. 2(a) is reliably preserved.

V. CONSEQUENCES

A wide variety of nonlinear oscillators were found to exhibit reliable synchronization when driven by either periodic or aperiodic inputs. This paper extends results for constant frequency drives to slowly fluctuating drives and provides analytical estimates for the conditions, rates, and the structural stability for synchronization of randomly driven phase oscillators. The application of the results of this adiabatic theory to the van der Pol oscillator with a moderate nonlinearity parameter ($\epsilon=1$) shows how these analytical results can predict the approximate conditions and rates of synchronization for randomly driven nonlinear oscillators that can be approximated by a phase model. These results suggest a useful way of thinking about the response of nonlinear oscillators to aperiodic inputs by demonstrating the close relationship to the periodically driven case. Specifically, the response of a nonlinear oscillator to a fluctuating input can be inferred from a thorough understanding of the asymptotic stability for periodic drives characterized by the Arnold tongue structures in the drive amplitude-frequency plane.

Although this paper was restricted to variable phase drives of the form $F(t)=B\sin\phi(t)$, similar results can be obtained for variable coupling, constant frequency drives of the form, $B(t)\sin\omega t$, and more generally for driving forces of the polar form, $F(t)=B(t)\sin\phi(t)$. As long as the transit time for the trajectory of the varying frequency, $\omega(t)$, and amplitude $B(t)$ through the stable zones is slow compared with the convergence rate, nearby oscillators will tend to synchronize.[24] In fact, because an arbitrary driving force can be conveniently decomposed into this polar form using Hilbert transforms,[25] the adiabatic theory can be extended to arbitrary driving forces.[24]

The final results for the strongly nonlinear ($\epsilon=4$), strongly driven van der Pol oscillator shown in Fig. 11 illustrate how effectively the adiabatic theory can be applied to estimate the conditions and rates of convergence even for driven nonlinear oscillators that are not well approximated by phase models. This result suggests a practical procedure for theoretically and experimentally evaluating the conditions and rates of synchronization for more general nonlinear oscillators with aperiodic driving forces. The idea is to carefully measure the response of the nonlinear oscillator to different periodic drives of the form $B\sin\omega t$ to map out the Arnold tongue structures in the $B-\omega$ parameter space, and then average these results over the statistical distributions that characterize the fluctuating drive.

In previous work[11] we have demonstrated that the nonlinear models used to model the spiking voltage dynamics of excitable cells, such as the Hodgkin–Huxley equations, can be synchronized with random driving currents and that the asymptotic stability of these biophysical models can account for the remarkable reliability of the spike-timing observed in experimental studies of the response of neocortical neurons to fluctuating current inputs.[12] Because asymptotic stability implies that two oscillators with different initial conditions will converge to the same response, repeated application of

the same drive to a single neuron will reliably generate the same response (even if the initial conditions are different). Moreover, the two responses will be virtually indistinguishable if the rate of convergence is faster than the natural spike frequency. Similar results have also been obtained for the reliable firing of Aplysia neurons subject to aperiodic drives[26] and this ''resonance effect'' has been successfully modeled using leaky integrate and fire models of the neuron.[26]

Another application of our analysis of the response of nonlinear oscillators to aperiodic drives is to the synchronization of chaotic systems. Chaotic dynamical systems are extremely sensitive to errors in initial conditions and parameters, so it was surprising that two nonlinear systems can be synchronized by a chaotically varying drive even with different initial conditions and small differences in parameters.[15] However, the present work shows that if the nonlinear systems exhibit asymptotic stability with strictly periodic drives, the conditions and rates for asymptotic stability with aperiodic (even chaotic) drives may be expected if the effective amplitude and frequencies of the aperiodic drive pass slowly through the stable zones for periodic drives.[27,28]

Finally, there has been great interest in the phenomenon of stochastic resonance in nonlinear oscillators where a single, nonresonant periodic drive is insufficient to cause mode-locking, but the addition of a moderate amount of broadband noise allows transient mode locking to the original periodic drive to occur, as evidenced by an enhanced peak in the power spectrum of the response of the driven system at the periodic frequency.[29,30] This effect is easily understood as an example of asymptotic stability in the presence of general aperiodic drives. In this case, the amplitude and frequency of the periodic drive alone is outside of the stable zones described by the Arnold tongues for the nonlinear oscillator. However, the addition of a moderate level of random forcing causes the effective amplitude and frequency of the drive to pass into the stable zones. As long as the random drive is not too strong to push the effective amplitude and frequency too quickly through the stable zones, the oscillator will exhibit transient mode locking at frequencies close to the original periodic frequency. For low amplitude noise the power spectrum of the periodically driven oscillator will continue to be peaked around the natural frequency. For moderate levels of noise a new peak will emerge at the frequency of the periodic drive, and for large amplitude noise this peak will diminish into a broadband background, thereby defining the stochastic resonance with a maximum response at a moderate level of random drive.

ACKNOWLEDGMENTS

Useful discussions with L. Abbott, W. Bialek, J. Cowan, B. Ermentrout, D. Selover, S. Strogatz, D. Tank, and A. Williamson and support from the NSF (IBN-9634409 and PHY-9900746) are gratefully acknowledged.

APPENDIX A: PARABOLIC FREQUENCY CHANGE

Figure 6(c) illustrates the two primary ways that the slowly varying drive frequency may traverse the stable zones of the periodically driven nonlinear oscillator. Between $t=10$ and 25 the instantaneous frequency, $\omega_r(t)$, traverses the stable zone twice almost linearly. At about $t=40$ and $t=60$, the drive frequency traverses an approximately parabolic path through the stable zone. The adiabatic theory for the linear case was treated in detail in Sec. III A. Here we will extend this analysis to a parabolically varying drive frequency.

Consider the case where the drive frequency, $\omega(t)=\omega_m-at^2$, first enters the stable zone at $t_0=-\sqrt{(b-(\Omega-\omega_m))/a}$, reaches a maximum (or minimum) frequency ω_m in the stable zone at $t=0$, and then leaves the stable zone at $t_f=\sqrt{(b-(\Omega-\omega_m))/a}$ after traversing a parabolic trajectory with curvature, $a/2$. In this case the solution to Eq. (16) is

$$\eta(t)=\arcsin\left[\frac{\Omega-(\omega_m-at^2)}{b}\right]+\xi(t), \tag{A1}$$

where Eq. (21) gives the approximate result for

$$\xi_\infty(t)=\frac{-2at}{b^2-(\Omega-\omega_m+at^2)^2}. \tag{A2}$$

This result for $\xi_\infty(t)$ is large at the edge of the stable zone, but vanishes at the apex of the parabola (at $t=0$). To estimate the typical size of $\xi_\infty(t)$, we can compute the value at the midpoint, halfway between the edge of the stable zone and the turning point, $t_m=\sqrt{(b/2-(\Omega-\omega_m))/a}$. Then $\xi_\infty(t_m)=-8\sqrt{(b/2-(\Omega-\omega_m))}a/3b^2$. If the drive frequency just reaches the natural frequency, $\omega_m=\Omega$, this estimate simplifies to $\xi_\infty(t_m)=-4\sqrt{2}a^{1/2}/3b^{3/2}$, which is small when $a^{1/2}/b^{3/2}\ll 1$.

As long as the transit time through the stable zone, $T=2\sqrt{(b-(\Omega-\omega_m))/a}$, is slow enough, nearby solutions will tend to converge with an average convergence rate of approximately

$$\begin{aligned}\Gamma &\approx \frac{1}{T}\int_{t_0}^{t_f}\sqrt{b^2-(\Omega-\omega_m+at^2)^2}\,dt \\ &\approx k\sqrt{b^2-(\Omega-\omega_m)^2},\end{aligned} \tag{A3}$$

where k is a constant of order unity (for $\omega_m=\Omega$, $k=\sqrt{\pi}\Gamma[1/4]/8\Gamma[7/4]\simeq 0.874$). As in the linear case, the corrections of order ξ_∞ to the instantaneous convergence rate tend to cancel upon integration over the transit time. Consequently, two nearby solutions will converge by a factor of $\exp[-k\sqrt{b^2-(\Omega-\omega_m)^2}T]$ during the transit time T through the stable zone. For $\omega_m=\Omega$, this convergence factor simplifies to $\exp(-2kb^{3/2}/a^{1/2})$, so that once again the condition that ξ_∞ is small, $a^{1/2}/b^{3/2}\ll 1$, is equivalent to the adiabaticity condition that the transit time convergence exponent is large.

APPENDIX B: STABILITY BOUNDARY FOR THE PERIODICALLY DRIVEN VAN DER POL OSCILLATOR

The estimate, Eq. (55), for the extent of the primary stable zone for the weakly nonlinear van der Pol oscillator was based on the approximate reduction to an equivalent phase model. This simple result agrees well with the more precise, but more complex derivations of the conditions for asymptotic stability for the weakly driven ($B\ll 1$), weakly nonlinear ($\epsilon\ll 1$) van der Pol oscillators with small detuning ($\Delta=|\Omega-\omega|\ll 1$) discussed in the literature.[4–6] These condi-

tions are determined by the simultaneous solutions of the equation for the average oscillator amplitude,[4–6]

$$(\tfrac{1}{4}a^3-a)^2+4a^2(\Delta/\epsilon)^2=(B/\epsilon)^2, \tag{B1}$$

and for the stability boundary,

$$(\tfrac{1}{2}-\tfrac{3}{8}a^2)(\tfrac{1}{2}-\tfrac{1}{8}a^2)+(\Delta/\epsilon)^2\geqslant 0. \tag{B2}$$

Here $\Delta=|1-\omega|$, because we can always rescale the time variable so that $\Omega=1$.[4–6] Moreover, when no simultaneous solution exists, Eq. (B2) is superseded by the auxiliary stability boundary

$$a\geqslant\sqrt{2}. \tag{B3}$$

If we eliminate $(\Delta/\epsilon)^2$ from Eqs. (B1) and (B2), we obtain a single equation for the critical amplitude a on the boundary of the stable zone,

$$a^4/2-a^6/8=(B/\epsilon)^2. \tag{B4}$$

Equation (B4) has a solution with $1.633<a<2$ as long as $B/\epsilon<1.089$. We can look for the simultaneous solutions of Eqs. (B1) and (B2) for a near 2 by substituting $a=2-\delta a$ into Eqs. (B1) and (B2) and deriving simultaneous conditions, $\delta a\approx(B/\epsilon)^2/8$ and $\delta a\approx 2(\Delta/\epsilon)^2$, from Eqs. (B1) and (B2), respectively, by neglecting small terms of order $(\delta a)^2$.

Equating these two results yields the same approximate condition for the boundary of the stability zone, $B=4\Delta$, that we have derived from the approximate phase model, Eq. (55). Roughly speaking when $B>4\Delta$, there exists a solution to Eq. (B1) with $a\geqslant 2$ so the stability condition in Eq. (B2) remains positive. However, when $B<4\Delta$, either there is no solution to Eq. (B1) with $a\approx 2$ or else the stability condition in Eq. (B2) goes negative. Moreover, when $B/\epsilon>1.089$, the critical value of the amplitude is simply determined by $a=\sqrt{2}$. In this case the stability boundary is determined by the constraint imposed by Eq. (B1) that $B\geqslant\sqrt{8\Delta^2+1/2}$, which also is in good agreement with the phase model estimate of $B\geqslant\sqrt{8}\Delta$ derived from by Eq. (51b) using $a(t)\approx\sqrt{2}$.

[a]Electronic mail: rjensen@wesleyan.edu

[1]C. Huygens, *Horologium Oscillatorium (1673)*, translated by R. Blackwell (Iowa U.P., Ames, IA, 1986), p. 30.
[2]G. B. Ermentrout and J. Rinzel, "Beyond a pacemaker's entrainment limit: Phase walk through," Am. J. Physiol. **246**, R102–R106 (1984).
[3]S. H. Strogatz, *Nonlinear Dynamics and Chaos* (Addison–Wesley, New York, 1994).
[4]C. Hayashi, *Nonlinear Oscillations in Physical Systems* (McGraw–Hill, New York, 1964).
[5]J. A. Murdock, *Perturbations: Theory and Methods* (Wiley, New York, 1991).
[6]D. W. Jordan and P. Smith, *Nonlinear Ordinary Differential Equations* (Clarendon, Oxford, 1987).
[7]R. He and P. G. Vaidya, "Analysis and synthesis of synchronous periodic and chaotic systems," Phys. Rev. A **46**, 7387–7392 (1992).
[8]A. S. Pikovskii, "Synchronization and stochastization of nonlinear oscillators by external noise" in *Nonlinear and Turbulent Processes*, edited by R. Z. Sagdeev (Harwood, New York, 1984), Vol. 3, pp. 1601–1604; "Synchronization and stochastization of the ensemble of autogenerators by external noise," Radiophys. Quantum Electron. **27**, 576–581 (1984).
[9]R. V. Jensen, "Synchronization of randomly driven nonlinear oscillators," Phys. Rev. E **58**, R6907–R6910 (1998).
[10]*Methods in Neuronal Modeling*, edited by C. Koch and I. Segev (MIT, Cambridge, MA, 1989).
[11]R. V. Jensen, L. Jones, and D. Gartner, "Synchronization of randomly driven nonlinear oscillators and the reliable firing of cortical neurons" in *Computational Neuroscience: Trends in Research, 1998*, edited by J. M. Bower (Plenum, New York, 1998), pp. 403–407.
[12]Z. F. Mainen and T. Sejnowski, "Reliability of spike timing in neocortical neurons," Science **268**, 1503–1506 (1995); A. C. Tang, A. M. Bartels, and T. Sejnowski, "Effects of cholinergic modulation on neocortical neurons in responses to fluctuating inputs," Cereb. Cortex **7**, 502–509 (1997).
[13]R. de Ruyter van Steveninck, D. Lewen, S. P. Strong, R. Koberle, and W. Bialek, "Reproducibility and variability in neural spike trains," Science **275**, 1805–1808 (1997); F. Rieke, D. Warland, R. de Ruyter van Steveninck, and W. Bialek, *Spikes: Exploring the Neural Code* (MIT, Cambridge, MA, 1997).
[14]See Focus Issue on Control and Synchronization of Chaos, Chaos **7**, 509–687 (1997).
[15]L. M. Pecora and T. L. Carroll, "Synchronization in chaotic systems," Phys. Rev. Lett. **64**, 821–824 (1990); L. M. Pecora and T. L. Carroll, "Driving systems with chaotic signals," Phys. Rev. A **44**, 2374–2383 (1991).
[16]K. M. Cuomo and A. V. Oppenheim, "Circuit implementation of synchronized chaos with applications to communications," Phys. Rev. Lett. **71**, 65–68 (1993).
[17]Y. Kuramoto, *Chemical Oscillations, Waves and Turbulence* (Springer, New York, 1984).
[18]See S. H. Strogatz, "Norbert Wiener's Brain Waves," in *Frontiers in Mathematical Biology*, edited by S. Levin, Lecture Notes in Biomathematics Vol. 100 (Springer-Verlag, New York, 1994), p. 122; "From Kuramoto to Crawford: exploring the onset of synchronization in populations of coupled oscillators," Physica D **143**, 1–20 (2000) for references to the most recent work on the synchronization of arrays of coupled nonlinear oscillators.
[19]See, for example, the classic work by R. L. Stratonovich, *Topics in the Theory of Random Noise* (Gordon and Breach, New York, 1967), Vol. 2.
[20]A. Papoulis, *Probability, Random Variables and Stochastic Processes* (McGraw–Hill, New York, 1965).
[21]S. O. Rice, in *Selected Papers on Noise and Stochastic Processes*, edited by N. Wax (Dover, New York, 1954), pp. 133–284.
[22]P. Hänggi and P. Riseborough, "Dynamics of nonlinear dissipative oscillators," Am. J. Phys. **51**, 347–352 (1983).
[23]R. C. Hilborn, *Chaos and Nonlinear Dynamics* (Oxford U.P., Oxford, 1994).
[24]R. V. Jensen (unpublished).
[25]M. G. Rosenblum, A. S. Pikovsky, and J. Kurths, "Phase synchronization of chaotic oscillators," Phys. Rev. Lett. **76**, 1804–1807 (1996).
[26]J. D. Hunter, J. G. Milton, P. J. Thomas, and J. D. Cowan, "Resonance effect for neural spike time reliability," J. Neurophysiol. **80**, 1427–1438 (1998).
[27]M. T. Roberts and R. V. Jensen (unpublished).
[28]P. C. Bressloff, J. D. Cowan, R. V. Jensen, and P. J. Thomas (unpublished).
[29]K. Wiesenfeld and F. Moss, "Stochastic resonance and the benefits of noise: From ice ages to crayfish and SQUIDs," Nature (London) **373**, 33–36 (1995).
[30]A. Longtin and D. R. Chialvo, "Stochastic and deterministic resonances for excitable systems," Phys. Rev. Lett. **81**, 4012–4015 (1998).